https://doi.org/10.48048/tis.2024.6882

FeTOMPP with Peroxidase-Like Activity as Peroxidase Mimics for Colorimetric Sensing of H_2O_2 and Ethanol

Jittima Khorungkul[1,*], Pariya Na Nakorn[1] and Supakorn Boonyuen[2]

[1]Department of Biotechnology, Faculty of Science and Technology, Thammasat University, Pathumthani 12121, Thailand
[2]Department of Chemistry, Faculty of Science and Technology, Thammasat University, Pathumthani 12121, Thailand

([*]Corresponding author's e-mail: jittimakho@gmail.com)

Received: 20 March 2023, Revised: 5 July 2023, Accepted: 27 July 2023, Published: 1 October 2023

Abstract

In this study, FeTOMPP (Tetrakis(4-methoxyphenyl) phenylporphyrinatoiron(III)) was synthesized and investigated for its peroxidase-like activity. The catalytic performance of FeTOMPP as a peroxidase mimic was explored by utilizing the colorless peroxidase substrate, 3,3',5,5'-tetramethylbenzidine (TMB), in the presence of hydrogen peroxide (H_2O_2). The oxidation of TMB by FeTOMPP resulted in the formation of its blue oxidized state. This enzymatic reaction was employed for the quantitative detection of H_2O_2, with a linear detection range spanning from 1.0 to 100 µM. The detection limit achieved using FeTOMPP as the catalyst was determined to be 2.4 µM. Furthermore, kinetic studies were conducted to investigate the interaction between FeTOMPP and H_2O_2. The results indicated that FeTOMPP exhibited favorable affinity towards H_2O_2, further highlighting its potential as a peroxidase mimic. In addition to its peroxidase-like activity, a simple and sensitive visual and colorimetric method was developed for the detection of ethanol by combining FeTOMPP with alcohol oxidase. The method relied on the use of TMB as the substrate. Ethanol-containing samples were subjected to the enzymatic reaction, resulting in the generation of a color change. The detection of ethanol was achieved with a minimum detection limit of 0.95 % v/v, and the linear range for quantification extended from 0 to 15 % v/v. This study demonstrates the potential application of FeTOMPP as a peroxidase mimic for the sensitive detection of H_2O_2 and the development of a colorimetric method for ethanol detection. The findings highlight the versatility and promising capabilities of FeTOMPP in various analytical and diagnostic applications.

Keywords: Porphyrin, Peroxidase, Colorimetric sensor, Hydrogen peroxide, Ethanol biosensor, Alcoholic beverage, Alcohol oxidase

Introduction

The practical application of natural enzymes as biocatalysts is often limited due to their lack of stability and loss of activation in harsh chemical environments [1-4]. Consequently, there has been a growing focus on the development of efficient enzyme mimetics to overcome these limitations. Peroxidase, a natural enzyme involved in physiological metabolism, exhibits highly efficient activation of oxides and peroxides, such as hydrogen peroxide (H_2O_2) [5,6]. H_2O_2 is not only a byproduct or intermediate in numerous biochemical reactions associated with biological processes but also a vital substance in pharmaceutical, biological, and environmental analyses [7]. However, the extraction of peroxidase poses challenges due to cost, storage difficulties, and susceptibility to environmental factors that can lead to a loss of activity [8,9]. Therefore, the synthesis and development of peroxidase mimics that can enhance their activity hold significant importance. In recent years, extensive efforts have been made to develop enzyme mimics, resulting in the emergence of various mimetics such as serine protease mimics [10] and cytochrome P450 mimetics [11]. Among these, peroxidase mimetics based on compounds like porphyrin [12], hematin [13,14], and hemin [15,16] have gained considerable attention for their potential in glucose and H_2O_2 detection [17]. However, the catalytic activity of these peroxidase mimics is still relatively inferior compared to natural enzymes [10]. Therefore, there is a continued need to design synthetic systems that can mimic natural enzymes while exhibiting high catalytic activity.

Porphyrins, as tetrapyrrole derivatives with their large conjugated electronic molecular structures, play a significant role in various scientific disciplines, including physics, chemistry, medicine, and biology [18]. In particular, they are closely associated with heme and hematin, which are important components of

peroxidase enzymes. These enzymes, such as the heme-containing enzyme HRP, as well as their mimetics, contain Fe^{2+} or Fe^{3+} ions within their active sites [19-22]. The ferric porphyrin units found in horseradish peroxidase (HRP) exemplify the presence of heme within peroxidase enzymes. It has been reported that heme-related compounds, such as haptoglobin, hemin and hematin exert anti-oxidative effect that hydrogen peroxide is one of the major oxidants [23]. Hui *et al.* (2022) have been reported that hemin, a porphyrin ring compound containing iron, had the peroxidase activity [24]. Therefore, porphyrins are interesting compounds to be tested as peroxidase mimetics because of their structural analogy with those of natural porphyrins.

In previous studies, researchers have explored the functionalization of porphyrins with materials like NiO, Fe_3O_4, and Co_3O_4 [25-27]. These functionalized porphyrins have exhibited enhanced peroxidase activity and have been capable of catalyzing reactions between dye substrates and H_2O_2, leading to color reactions that can be visually observed. This highlights the potential of porphyrin-based systems for mimicking peroxidase activity and their ability to perform catalytic reactions in the presence of hydrogen peroxide.

Alcohol monitoring demands highly sensitive, cost-effective, and selective detection systems. To address this need, we have devised a novel approach for ethanol detection by combining the catalytic reaction of ethanol with alcohol oxidase (AOX) and the peroxidase-like catalytic reaction of a porphyrin mimetic. In this study, we extensively characterized the peroxidase-like catalytic properties of the porphyrin mimetic and observed its strong affinity towards the substrate. Building upon these findings, we have developed a colorimetric method for the quantitative analysis of both H_2O_2 and ethanol. This method holds great promise for its ability to accurately detect and measure ethanol levels while offering the advantages of sensitivity, cost-effectiveness, and selectivity required for current and future alcohol monitoring applications.

Materials and methods

Reagents

All chemicals used in this study were of analytical grade without further purification. Hydrogen peroxide (H_2O_2, 30 wt.%, acetic acid (HAc), sodium acetate (NaAc), ethanol**,** Succinic acid, ascorbic acid, acetic acid, lactic acid, oxalic acid, sodium sulfite, 3,3',5,5'-tetramethylbenzidine (TMB) and alcohol oxidase were purchase from Sigma-Aldrich. Malic acid and tartalic acid were purchased from Supleco. Citric acid was from Chemipan corporation (Thailand). FeTOMPP was from analytical chemistry laboratory, Thammasart University (Thailand).

Instruments

The FT-IR (4,000 - 400 cm^{-1}) spectra were recorded on Perkin Elmer infrared spectrophotometer (spectrum GX). Mass spectra were obtained on Thermo Finnigan mass spectrometer (LCQ Advantage). The elemental analysis was carried out on Perkin Elmer (2,400) elemental analyzer. UV-Vis absorption was carried out on a UV Visible spectrophotometer Biochrom Libra S80 model. GC were analyzed on Shimadzu GCMS-TQ series.

Preparation of iron(III) porphyrin (FeTOMPP)

The free base porphyrin 5,10,15,20-tetrakis(4-buthyloxyphenyl)porphyrin was prepared as previously reported [28]. The Fe(III) porphyrin was synthesized with the corresponding free base, as previously reported. The tetrakis(4-methoxyphenyl) phenylporphyrinatoiron(III) (FeTOMPP) was obtained as purple crystal in 73 % yield. FTIR (KBr, cm^{-1}): 2,943, 1,581 (C-H stretch), 1,462, 1,350 (C=C stretch), 1,237 (C-N stretch), 1,125 (C-O stretch), and 812 (C-H bend). Mass *m/z* (ESI) calculated for FeC50H41O6N4: 775.58 measured: 782.4 (M+H).

Preparation of samples

Iron(III) porphyrin solutions was prepare by dissolving FeTOMPP in dimethylsulfoxide (DMSO) at 0.1 - 0.8 mg/mL. The stock solutions were then diluted with sodium acetate to obtain concentration of DMSO at 1 % (v/v) and concentration of FeTOMPP 10 - 80 µg/mL.

UV-visible absorbance measurements

The peroxidase-like activity of FeTOMPP was measured by catalytic oxidation of peroxidase substrate TMB in the presence of H_2O_2. The experiments were carried out by using FeTOMPP in a reaction volume of 2.0 mL with 500 µM TMB and 100 µM H_2O_2 as substrates. The colorimetric analysis was

prepared as follows: 200 µl of TMB (5 mM), 200 µl of FeTOMPP stock solution (50 µg/mL), and 200 µl of H_2O_2 (1 mM) were added into 1.4 mL of sodium acetate (NaAc) buffer (0.1 mM, pH 6). The reaction is incubated at 30 °C for 10 min. The concentration of the oxidized TMB was quantified by UV-Vis absorption spectroscopy at 652 nm by using a molar extinction coefficient of ε = 3.9×104 M^{-1} cm^{-1} [25].

The optimum conditions (FeTOMPP amount, pH and temperature) were measured by using variation amount of FeTOMPP (0 - 80 µg) (200 µl from stock solution) in 1.4 mL sodium acetate (NaAc) buffer (0.1 mM, pH 2 - 10) in the presence of H_2O_2 (1 mM) as the substrates, TMB concentration was 500 µM and the total reaction volume was 2 mL. The reaction was incubated at 25 - 50 °C for 10 min. The concentration of the oxidized TMB is quantified by UV-Vis absorption spectroscopy at 652 nm.

The Michaelis-Menten constant was calculated by using Lineweaver-Burk plots of the double reciprocal of the Michaelis-Menten equation:

$$\frac{1}{v} = \frac{Km}{Vm} \times \left(c + \frac{1}{km}\right)$$

where ν is the initial velocity, ν_m represents the maximal reaction velocity, C corresponds to the concentration of substrate, and K_m is the Michaelis constant.

Detection of H_2O_2

The detection for H_2O_2 was carried out as follows. 200 µl solution contained different amounts of H_2O_2 was added into a 0.1 mM NaAc buffer (pH 6.0) with 500 µM and FeTOMPP in a total volume of 2 mL. The resulted solution was incubated at 30 °C before UV-Vis measurements. The linear range and detection limit were also quantified. The sensing colorimetric mechanism for H_2O_2 was schematic illustrated in **Scheme 1**.

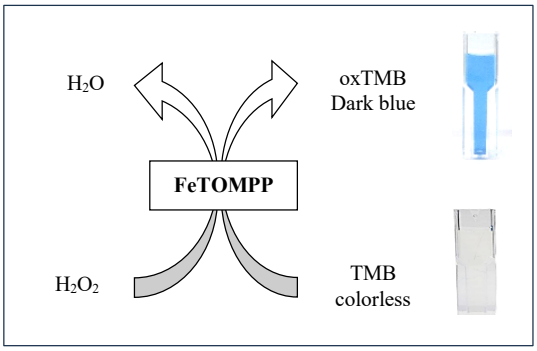

Scheme 1 Schematic illustration of oxidation color reaction of TMB in the presence of H_2O_2 catalyzed by porphyrin mimetic peroxidase.

Detection of ethanol

10 µl alcohol oxidase was added into a 0.1 M phosphate buffer solution (PBS, pH 7.0) containing different amounts of ethanol and incubated at 37 °C for 20 min. After that, the above solution was added into a 0.1 M NaAc buffer (pH 6.0) containing 500 µM TMB and FeTOMPP in a total volume of 2 mL. The resulted solution was incubated at 30 °C before UV-Vis measurements and was used for standard curve. The linear range and detection limit were also quantified.

Interference measurement

Succinic acid, ascorbic acid, acetic acid, lactic acid, malic acid, oxalic acid, citric acid, tartaric acid, and sodium sulfite were checked as potential interferences with the color change of the system response. The interferences sample were dilute 1:10 in phosphate buffer 0.1 M pH 7. The reaction solution was added with percent ratio 2:1 interference (2 % v/v): ethanol (1 % v/v) in the total volume of 2 mL. The resulted solution was quantified by UV-measurement.

Real sample measurement

Samples of local and market alcoholic beverages were bought. 100 µl of sample was added into a mixture of AOX and 0.1 M PBS (pH 7.0) and incubated at 37 °C for 20 min. After that, the solution was added into a mixture of 0.1 mM NaAc buffer (pH 6.0), 500 µM TMB and FeTOMPP in a total volume of

2 mL. The resulted solution was quantified by UV-Vis measurement and compare to the standard curve to indicate the ethanol concentration.

Gas chromatographic measurement [29]

For comparison purposes, local and market alcoholic beverages samples were also analyzed by gas chromatography with Shumadzu GCMS-TQ chromatograph composed of an injector and flame ionization detector (FID). Automated injection with DB-1 column, 0.25 nm I.D. ×30 m length ×3 µm film thickness. The alcoholic beverages are analyzed using internal standard method. A calibration plot for ethanol in concentrations ranging between 1.0 and 10 % (v/v) was constructed using 5 % of isopropanol as internal standard. The samples are previously diluted to obtain an adequate ethanol concentration.

Results and discussion

Synthesis and characterization of iron(III) porphyrin

Free base porphyrin (TOMPP) was synthesized according to Alder's method [30]. The Fe(III) porphyrin was formed by the reaction of iron acetate with TOMPP in the presence of sodium acetate in acetic acid (**Scheme 2**). After separation using SGCC and 5:1 (v/v) DCM:MeOH, the Fe(III) porphyrin was obtained in 73 % yield.

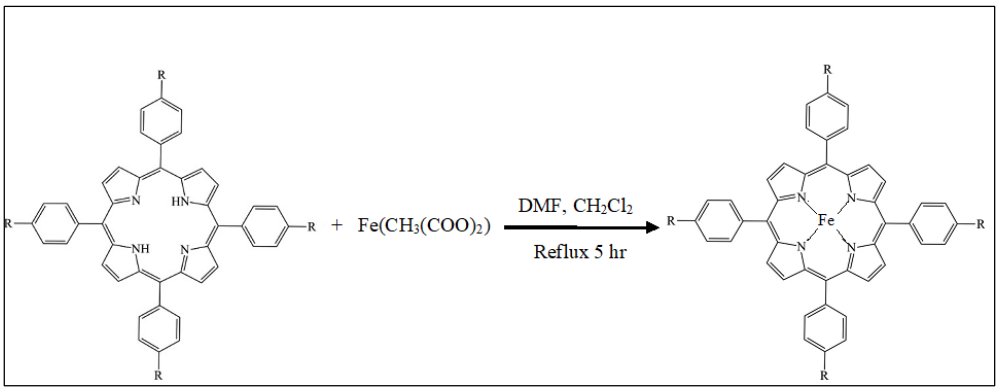

Scheme 2 Preparation of Iron(III) porphyrin.

The peroxidase-like activity of FeTOMPP

Porphyrins, including heme, are natural compounds known for their various biological activities. Among them, heme stands out as one of the most abundant porphyrins. It has been observed that heme-related compounds, such as haptoglobin, hemin, and hematin, exhibit antioxidative effects against hydrogen peroxide, which is a major oxidant [23]. In a study conducted by Hui *et al.* (2022), it was reported that hemin, a porphyrin ring compound containing iron, displayed peroxidase activity [24]. These findings highlight the potential of porphyrins as peroxidase mimetics due to their structural similarity to natural porphyrins.

To assess the peroxidase-like activity of FeTOMPP, a reaction mixture was prepared by adding 50 µg/mL of FeTOMPP stock solution in sodium citrate (NaAc) buffer (0.1 mM, pH 6). The substrates used in the reaction were 500 µM of TMB and varying amounts of H_2O_2 (50-200 µM). The total reaction volume was 2 mL, and the mixture was incubated for 10 min. The peroxidase-like activity of FeTOMPP was evaluated based on the oxidation of TMB in the presence of H_2O_2. TMB, which is initially colorless, undergoes oxidation in the presence of peroxidase or compounds with peroxidase-like activity, resulting in the formation of the blue oxidized form of TMB (oxTMB) (**Figure 1**). The formation of oxTMB was confirmed using UV-Vis absorption spectroscopy [31]. The resulting blue solution exhibited characteristic absorption peaks at 375 and 652 nm, corresponding to the absorption peaks of oxTMB [32-34]. These absorption peaks served as indicators of the peroxidase or peroxidase-like activity of the tested compounds. The obtained results, shown in **Figure 1**, revealed that FeTOMPP catalyzed the oxidation of TMB, leading to the generation of a blue color. This observation demonstrated that FeTOMPP exhibited peroxidase-like activity towards a typical peroxidase substrate. FeTOMPP was Fe(III) porphyrin complex similar to hemin which is protoporphyrin IX containing a ferric iron. Thus, FeTOMPP would have the peroxidase activity and selected for further study.

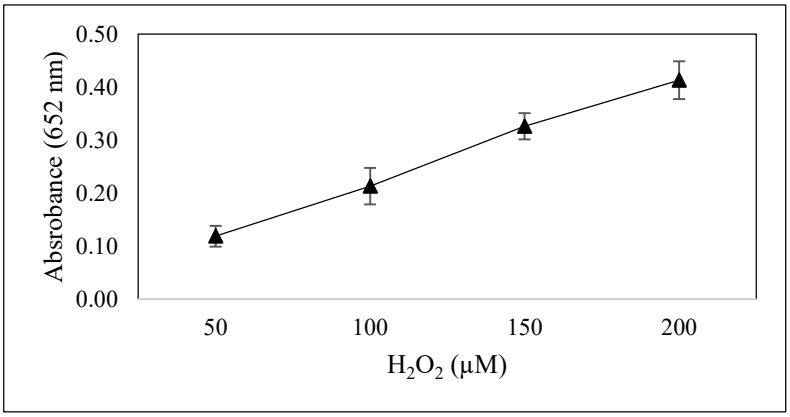

Figure 1 peroxidase-like activity of FeTOMPP with different concentration of H_2O_2.

The determination of the optimal amount, pH, and temperature of FeTOMPP was based on the highest absorbance observed in the reaction, as depicted in **Figure 2**. The optimal conditions were found to be 35 μg/mL FeTOMPP, pH 6, and a temperature of 30 °C. Therefore, pH 6 and 30 °C were selected as the standard conditions for the subsequent analysis of FeTOMPP's catalytic activity. Furthermore, it was observed that the catalytic activity of FeTOMPP was significantly higher under weakly acidic conditions compared to neutral conditions. This finding suggests that the oxidation reaction of TMB readily occurred under weakly acidic conditions, similar to other synthetic porphyrins [26, 35, 36], and the natural enzyme HRP [37].

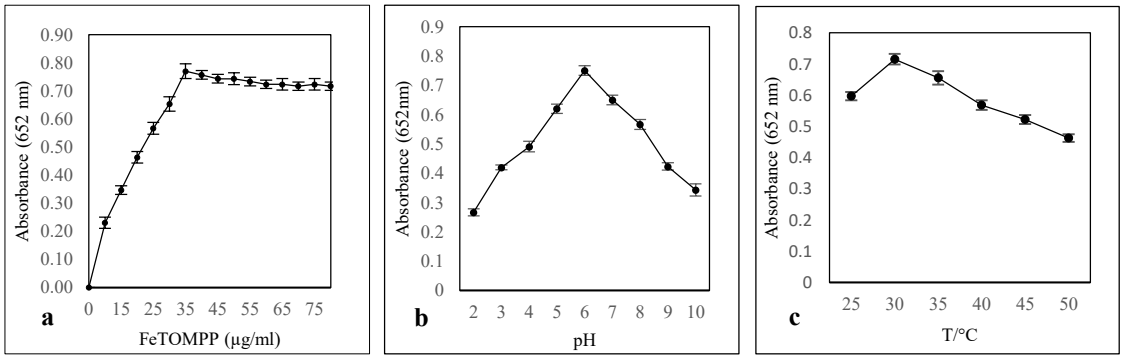

Figure 2 Effect of (a) amount of FeTOMPP, (b) pH, and (c) temperature on the absorbance of oxTMB at 652 nm.

Detection of H_2O_2

The feasibility of utilizing FeTOMPP for the determination of H_2O_2 in the presence of TMB was investigated based on the UV-Vis absorbance at 652 nm. The results, depicted in **Figure 2**, revealed a linear increase in UV-Vis absorbance as the concentration of H_2O_2 increased from 1.0 to 1.0 mM, accompanied by a gradual color change to blue. The **Figure 3(b)** presents the calibration curve for H_2O_2, covering a concentration range of 1 to 100 μM. The color variations observed in the oxidation of TMB catalyzed by FeTOMPP were found to be dependent on the concentration of H_2O_2. The absorbance at 652 nm (Y) displayed a linear correlation with the concentration of H_2O_2 (X) in μM, as depicted by the calibration curve. The equation describing this relationship was determined to be $Y = 0.0013 + 0.0022X$, with a high linear correlation coefficient (R) of 0.997. The detection limit of the assay was determined to be 2.4 μM. Notably, this detection limit surpassed that of many other H_2O_2 sensors reported in the literature [34,38,39]. Furthermore, the linear range achieved by the FeTOMPP-based system was wider compared to previous studies [40-44]. These changes in color were also discernible to the naked eye, allowing for convenient visual detection of H_2O_2 concentration levels.

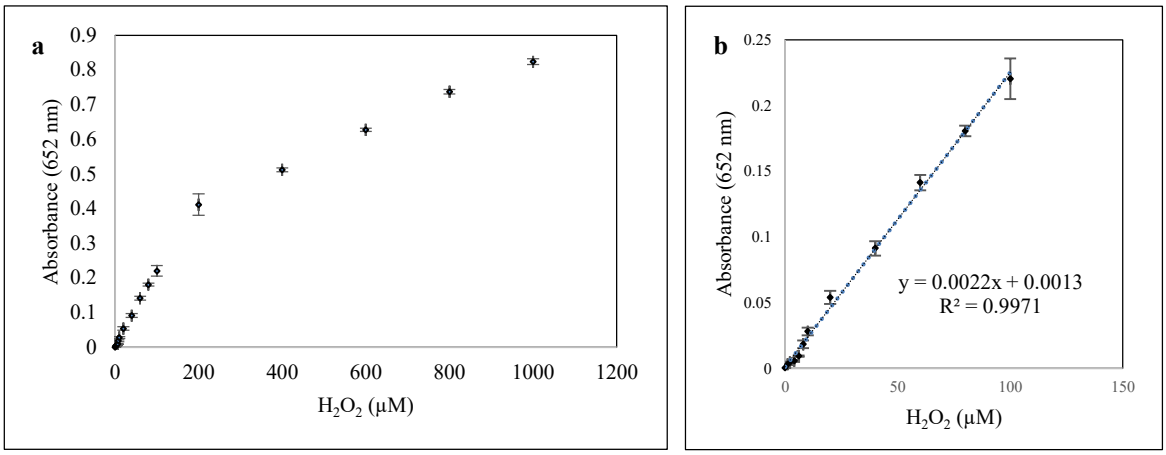

Figure 3 a Linear calibration plot of oxTMB in the presence of FeTOMPP and different concentration of H_2O_2 ranging from 1.0 μM to 1.0 mM. and b The calibration curve for H_2O_2, covering a concentration range of 1 to 100 μM.

Steady-state kinetic assays

To analyze the catalytic mechanism and acquire kinetic parameters, the catalytic activity of FeTOMPP was studied the enzyme kinetics theory and methods with H_2O_2 and TMB as substrates (**Figure 4**). A series of experiments were performed by changing the concentration of 1 substate and keeping the concentration of the other constant. The maximum initial velocity (V_m) and Michaelis-Menten constant (K_m) were calculated from Lineweaver-Burk plots and are list in **Table 1**.

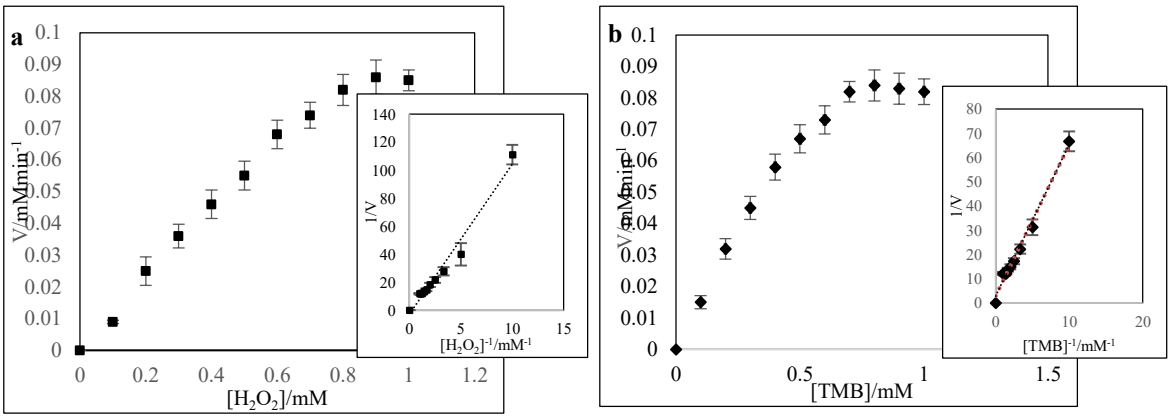

Figure 4 Steady-state kinetic assays of the FeTOMPP. A The concentration of H_2O_2 was 400 μM and TMB concentration was varied. and b The concentration of TMB was 500 μM and H_2O_2 was varied.

Table 1 Comparison of the apparent Michaelis-Menten constant (K_m) and maximun reaction rate (V_m).

Catalyst	Vm(10^{-8}Ms^{-1})		Km(mM)	
	TMB	H_2O_2	TMB	H_2O_2
FeTOMPP	0.278	8.54	3.74	2.15
HRP	0.434	3.70	13.08	5.31

The Michaelis constant (Km) is widely used as a measure of enzyme-substrate affinity, with a smaller Km value indicating a stronger binding between the enzyme and substrate. In our study, we investigated the Km values of FeTOMPP for H_2O_2 and TMB, and compared them with those of HRP, as shown in **Table 3** [37]. The results revealed that FeTOMPP exhibited a smaller Km value (2.15 mM) for H_2O_2, indicating a higher affinity for H_2O_2 compared to HRP. On the other hand, FeTOMPP showed a larger Km value

(3.74) for TMB, suggesting a weaker affinity between FeTOMPP and TMB compared to HRP. This difference in Km values further supports the notion that FeTOMPP possesses good catalytic activity towards H_2O_2 when compared to HRP. Additionally, we evaluated the maximum velocity (Vm) of FeTOMPP for both H_2O_2 and TMB, and found that it was larger than that of HRP, as shown in **Table 1**. This indicates that FeTOMPP exhibits an enhanced catalytic activity for both H_2O_2 and TMB. Overall, our findings demonstrate the favorable enzymatic properties of FeTOMPP, particularly its strong affinity for H_2O_2 and improved catalytic activity compared to HRP.

Stability test of the system

The tested system was prepared as stock solution that contained dissolved FeTOMPP, 0.1 mM NaAc buffer (pH 6.0) and 500 μM TMB and kept at room temperature without contact with light. The pH of the solution was measured every day and before tested. To test the stability of the system, TMB-H_2O_2 were measured by using the stock solution stored for different days (0 - 15 days) as catalyst and the concentration of H_2O_2 was 100 μM. The concentration of the oxidized TMB was quantified by UV-Vis absorption spectroscopy at 652 nm. The results showed that the absorbance at 652 nm almost did not vary (less than 5 %) as shown in **Figure 5**. The pH of the stock solution was measured and found that from day 1 to 15 the pH of the solution almost did not change as shown in **Figure 5**.

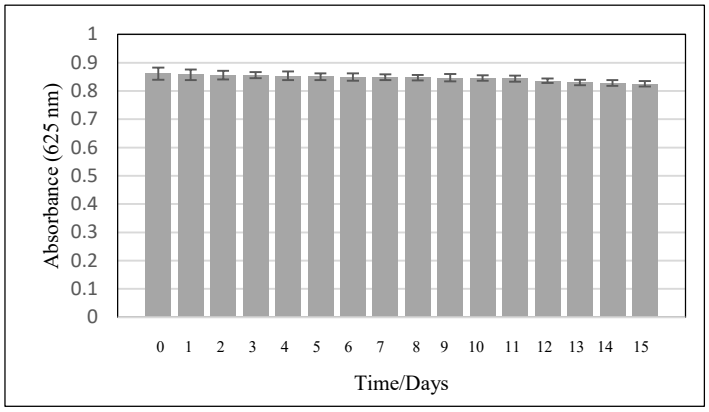

Figure 5 The absorbance at 652 nm of FeTOMPP-TMB-H_2O_2 stored for different days as catalyst (the concentration of H_2O_2 is 1 mM).

Detection of ethanol

As H_2O_2 is the main product of alcohol oxidase (AOX)-catalyzed reaction. When combined with the alcohol catalytic reaction by alcohol oxidase (AOX), a colorimetric method for ethanol detection can be realized by utilizing the same chromogenic substrate TMB and TMB-H_2O_2 catalyzed color reaction. Therefore, the enzymatic reaction could be monitored optically by the reduction of TMB from its colorless color to dark blue color as shown in **Scheme 3**.

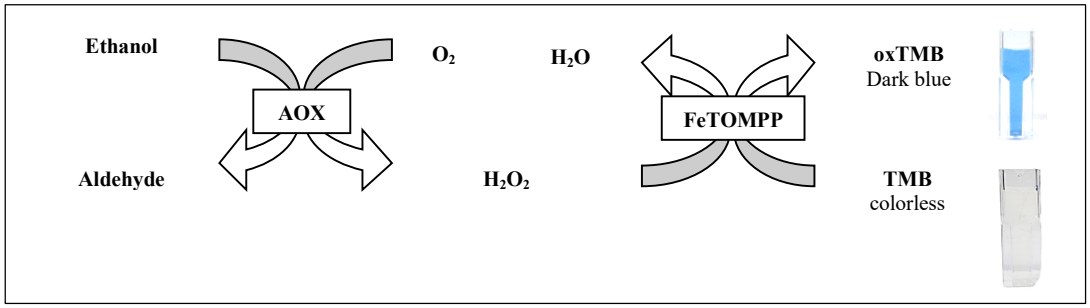

Scheme 3 Illustration detection mechanism for H_2O_2 and ethanol sensing using FeTOMPP and AOx.

In our previous experiment, we demonstrated that FeTOMPP could be utilized to quantify the concentration of H_2O_2 in the presence of TMB. Building upon this, we explored the catalytic reaction of ethanol with alcohol oxidase (AOX) in the presence of FeTOMPP and TMB. To initiate the reaction, 10 μl of AOX was added to 0.1 M phosphate buffer solutions (PBS, pH 7.0) containing varying concentrations

of ethanol. The mixture was then incubated at 30 °C for 20 min. Subsequently, the solution was combined with a 0.1 mM NaAc buffer (pH 6.0) containing 500 µM TMB and a stock solution of FeTOMPP, resulting in a total volume of 2 mL. The resulting solution was incubated at 30 °C prior to UV-Vis measurements. As depicted in **Figure 6**, the absorbance at 652 nm exhibited a linear increase within a specific range of ethanol concentration. This linear relationship between the absorbance and ethanol concentration was observed in the range of 0 - 15 % v/v, with a detection limit of 0.80 % v/v. These results highlight the potential of this method for accurate and sensitive detection of ethanol concentration using FeTOMPP in conjunction with TMB.

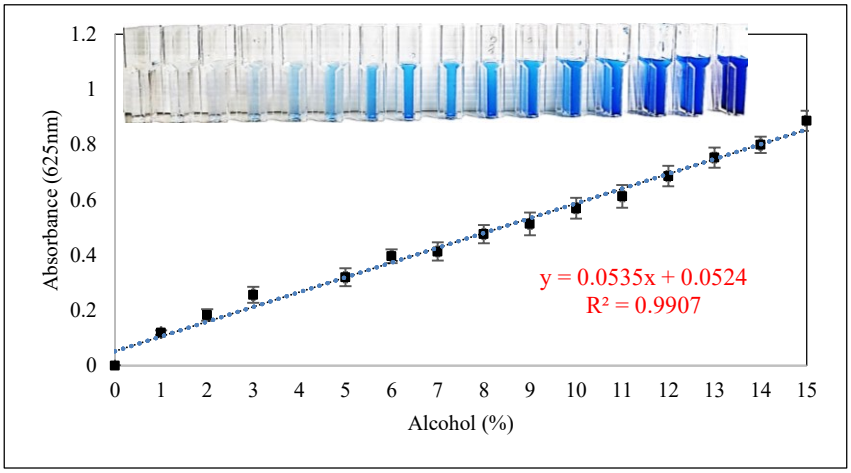

Figure 6 linear calibration plot of oxTMB in the presence of FeTOMPP and different concentration of alcohol ranging from 0 - 15 %.

Interferences measurement

During the fermentation of some traditional alcoholic beverages, some organic acids were present. Luangkhlapho *et al.* (2013), report that citric acid, succinic acid, lactic acid, acetic acid, and glycerol were detected by HPLC in the Sato product using different source of Loogpang [45]. Tartaric acid, malic acid, citric acid, succinic acid, lactic acid and acetic acid were organic acid commonly found in Wine product [46]. Tartaric acid and Malic acid commonly found in many fruits including apples and grapes. [47,48]. Citric acid is an intermediate of the TCA cycle and is widespread in nature, while succinic acid, lactic acid and acetic acid were organic acid derived from fermentation [46]. Succinic acid, ascorbic acid, acetic acid, lactic acid, malic acid, oxalic acid, citric acid, tartaric acid, and sodium sulfite were checked as potential interferences with the color change of the system response. The results obtained were present in **Table 2**.

Table 2 Interference of some compounds; % ratio 2:1 interference (2 % v/v); ethanol (1 % v/v), on the response to ethanol of biosensors.

Compound	Response of the biosensor
Succinic acid	97.5 ± 0.408
Ascorbic acid	99 ± 0.624
Acetic acid	98.5 ± 0.408
Lactic acid	99 ± 0.408
Malic acid	97 ± 0.816
Oxalic acid	99 ± 0.624
Citric acid	96 ± 0.624
Tartaric acid	96.5 ± 0.408
Sodium sulphite	98.5 ± 0.408

In addition to ethanol, organic acids are commonly found in beverage samples and can potentially interfere with the analysis. It has been reported that the chemical reaction between organic acids and oxygen can lead to a decrease in the current of amperometric biosensors [49]. To investigate the potential interference of organic acids on ethanol biosensors, Wen *et al.* [50] conducted a study where they examined the decrease in oxygen levels and calculated it as an equivalent ethanol concentration. The results of their

study indicated that the presence of organic acids had negligible or minimal interference on the ethanol biosensor based on bacteria.

In our own experiments (**Table 3**), we evaluated the interference of organic acids and sodium sulphite on the sensor response to ethanol. We observed a slight decrease in the sensor response in the presence of these interferents, but the interference was found to be minimal, with values below 5 %. The reduced sensor response can be attributed to the oxidation of the interferents, which affects the activity of alcohol oxidase (AOX). These findings further support the suitability of our approach using FeTOMPP and TMB for the accurate detection of ethanol concentration, as the interference from organic acids is minimal and does not significantly impact the sensor response.

Ethanol analysis in fermented beverage samples

The determination of ethanol in alcoholic beverages were carried out. Some different alcoholic beverages were purchase from the market and analyzed the ethanol value using the developed biosensor. The pretreatment of these samples only requires a dilution step. Each sample was diluted with phosphate buffer 0.1 M pH 7 to a concentration within the working range of the biosensor. This procedure can also reduce the interference effect. The ethanol content of all types of fermented beverage samples was measured and summarized results are given in **Table 3**. The biosensor accuracy was assessed by comparison with the results given by the beverage producers and others with the gas chromatography method.

From the results the ethanol value in different alcoholic beverage analyzed by GC and the sensor were not much vary (less than 5 %). Then this sensor could be reliable and could be used to analyze ethanol in fermented beverage samples.

Table 3 Determination of ethanol in the fermented beverage samples with porphyrin biosensor and by applying GC. Data are given as average ± SD (n = 3).

Beverage samples	Ethanol (%v/v)		
	Value declared by the producer	GC	Biosensor
Beer 1	6.4	6.35 ± 0.012	6.10 ± 0.2
Beer 2	5.5	5.50 ± 0.012	5.35 ± 0.1
Beer 3	5.0	5.10 ± 0.06	4.95 ± 0.08
Beer 4	5.0	5.17 ± 0.08	4.95 ± 0.08
Sato 1	-	11.0 ± 0.06	10.50 ± 0.2
Sato 2	-	7.10 ± 0.012	6.8 ± 0.1
Sato 3	6.5	6.4 ± 0.08	6.3 ± 0.05
Krachae	-	9.0 ± 0.06	8.8 ± 0.15
Soju 1	13	12.8 ± 0.012	12.2 ± 0.2
Soju 2	14	14 ± 0.08	13.5 ± 0.5
Wine 1	5	4.9 ± 0.012	4.65 ± 0.08
Wine 2	5	4.65 ± 0.08	4.5 ± 0.1
Wine 3	11.5	11.5 ± 0.06	11 ± 0.2
Liquor 1	40	41.56 ± 0.012	40 ± 0.5
Liquor 2	40	39.23 ± 0.08	39 ± 0.15

Conclusions

The peroxidase-like property of FeTOMPP was investigated and showed a higher affinity to H_2O_2 than the natural enzyme HRP. On this basis, a simple and visual colorimetric method to detect H_2O_2 and ethanol was developed successfully. The result exhibited a reasonable linear range and detection limit with high sensitivity, stability and selectivity. Furthermore, this method was applied to detect ethanol in alcoholic beverage and showed good ability, so it was promising in alcohol measurement.

Acknowledgements

This work was supported by Thammasart University, Thailand and Valaya Alongkorn Rajabhat University, Thailand. The authors are also thankful to Science Center of Valaya Alongkorn Rajabhat University, Thailand for providing the equipment for this research.

References

[1] LZ Gao, J Zhuang, L Nie, JB Zhang, Y Zhang, N Gu, TH Wang, J Feng, D Yang, S Perrett and X Yan. Intrinsic peroxidase-like activity of ferromagnetic nanoparticles. *Nat. Nanotechnol.* 2007; **2**, 577-83.

[2] JM Perez. Iron oxide nanoparticles: Hidden talent. *Nat. Nanotechnol.* 2007; **2**, 535-6.

[3] MJ Banholzer, JE Millstone, L Qin and CA Mirkin. Rationally designed nanostructures for surface enhanced ramen spectroscopy. *Chem. Soc. Rev.* 2008; **37**, 885-97.

[4] L Zhang, Q Zhang and J Li. Layered titanate nanosheets intercalated with myoglobin for direct electrochemistry. *Adv. Funct. Mater.* 2007; **17**, 1958-65.

[5] M Filizola and GH Loew. Role of protein environment in horseradish peroxidase compound I formation: Molecular dynamics simulations of horseradish peroxidase-HOOH complex. *J. Am. Chem. Soc.* 2000; **122**, 18-25.

[6] JN Rodriguez-Lopez, DJ Lowe, J Hernadez-Ruiz, ANP Hiner, F Gracia-Canovas and RNF Thorneley. Mechanism of reaction of hydrogen peroxide with horseradish peroxidase: Identification of intermediates in the catalytic cycle. *J. Am. Chem. Soc.* 2001; **123**, 11838-47.

[7] F Yin, Hk Shin and YS Kwon. A hydrogen peroxide biosensor based on langmuir-blodgett technique: Direct electron transfer of hemoglobin in octadecylamine layer. *Talanta* 2005; **67**, 221-6.

[8] G Wulff. Enzyme-like catalysis by molecularly inprinted polymers. *Chem. Rev.* 2002; **102**, 1-28.

[9] E Shoji and MS Freund. Potentiometric saccharide detection based on the pK_a changes of poly (aniline boronic acid). *J. Am. Chem. Soc.* 2002; **124**, 12486-94.

[10] F Qin, S Jia, F Wang, S Wu, J Song and Y Liu. Hemin@metal-organic framework with peroxidase-like activity and its application to glucose detection. *Catal. Sci. Tech.* 2013; **3**, 2761-8.

[11] SP Visser. Preferential hydroxylation over epoxidation catalysis by a horseradish peroxidase mutant: A cytochrome P450 mimic. *J. Phys. Chem. B* 2007; **111**, 12299-302.

[12] W Zhong-Shuai, L Chen, J Liu, K Parvez, H Liang, J Shu, H Sachdev, R Graf, X Feng and K Müllen. High-performance electrocatalysis for oxygen reduction derived from cobalt porphyrin-based conjugated mesoporous polymer. *Adv. Mater.* 2014; **26**, 1450-5.

[13] D Hu, Y Song and L Wang. Nanoscale luminescent lanthanide-based metal-organic-framework: Properties, synthesis, and application. *J. Nanoparticle Res.* 2015; **17**, 310-5.

[14] Q Hu, W Hu, J Kong and X Zhang. Ultrasensitive electrochemical DNA biosensor: By hematin as efficient biomimetic catalyst toward in situ metallization. *Biosens. Bioelectron.* 2015; **63**, 269-75.

[15] Q Wang, Z Yang, X Zhang, X Xiao, CK Chang and B Xu. A supramolecular-hydrogel-encapsulated hemin as an artificial enzyme to mimic peroxidase. *Angew. Chem. Int. Ed. Engl.* 2007; **46**, 4285-9.

[16] L Furk and CM Niemeyer. Covalent hemin-DNA adducts for generating a novel class of artificial heme enzymes. *Angew. Chem. Int. Ed. Engl.* 2005; **44**, 2603-6.

[17] WC Ellis, CT Tran, MA Denardo, A Fischer, AD Ryabov and TJ Collins. Design of more powerful iron-TAMI peroxidase enzyme mimics. *J. Am. Chem. Soc.* 2009; **131**, 18052-3.

[18] K Kadish, KM Smith and R Cuilard. *The porphyrin handbook.* Academic Press, New York, 1999, p. 152-60.

[19] A Henriksen, A Smith and M Gajhede. The structures of the horseradish peroxidase c-ferulic acid complex and ternary complex with cyanide suggest how peroxidase oxidize small phenolic substrates. *J. Biol. Chem.* 1999; **274**, 35005-11.

[20] M Kvaratskhelia, C Winkel and R Thorneley. Purification and characterization of a novel class III peroxidase isoenzyme from tea leaves. *Plant Physiol.* 1997; **114**, 1237-45.

[21] K Kariya, E Lee, M Hirouchi, M Hosokawa and H Sayo. Purification and some properties of peroxidases of rat bone marrow. *Biochim. Biophys. Acta* 1987. **911**, 95-101.

[22] M Mathy-Hartert, E Bourgeois, S Grulke, G Deby-Dupont, I Caudron, C Deby, M Lamy and D seryn. Purification of myeloperoxidase from equine polymorphonuclear leucocytes. *J. Vet. Res.* 1998; **62**, 127-32.

[23] I Vlasova. Peroxidase activity of human hemoproteins: keeping the fire under control. *Molecules* 2018; **23**, 2561-88.

[24] T Somboon and S Sansuk. An instrument-free method based on visible chemical waves for quantifying the ethanol content in alcoholic beverages. *Food Chem.* 2018; **23**, 300-4.

[25] W Hui, Z Yan, K Fang, M Wu, W Mu, C Zhao, D Xue, T Zhu, X Li, M Gao, Y Lu and K Yan. Hemin with peroxidase activity can inhibit the oxidative damage induced by ultraviolet A. *Curr. Issues Mol. Biol.* 2022; **44**, 2683-94.

[26] Q Liu, Y Yang, H Li, R Zhu, Q Shao, Z Yang and J Xu. Nio nanoparticles modified with 5,10,15,20-tetrakis(4-carboxyl phenyl)-porphyrin: Promising peroxidase mimetics of H_2O_2 and glucose detection. *Biosens. Bioelectron.* 2015; **64**, 147-53.

[27] Q Liu, L Zhang, H Li, Q Jia, Y Jiang, Y Yang and R Zhu. One-pot synthesis of porphyrin functionalized γ-Fe_2O_3 nanocomposites as peroxidase mimics for H_2O_2 and glucose detection. *Mater. Sci. Eng. C* 2015; **55**, 193-200.

[28] Q Liu, R Zhu, H Du, Y Yang, Q Jia and B Bian. Higher catalytic activity of porphyrin funtionalized Co_2O_4 nanostructures for visual and colorimetric detection of H_2O_2 and glucose. *Mater. Sci. Eng. C* 2014; **43**, 321-9.

[29] KH Chow, RW Sun, JB Lam, CK Li, A Xu, DL Ma, R Abagyan, Y Wang and CM Che. A gold(III) porphyrin complex with antitumor properties targets the Wnt/β-catenin pathway. *Canc. Res.* 2010; **70**, 329-37.

[30] AD Alder, FR Longo and W shergalis. Mechanistic investigations of porphyrin syntheses. I. Preliminary studies on ms-tetraphenylporphin. *J. Am. Chem. Soc.* 1964; **86**, 3145-9.

[31] H Tan, C Ma, L Gao, Q Li, Y Song, F Xu, H Tan, C Ma, L Gao, Q Li, Y Song, F Xu, T Wang and L Wang. Metal-organic framework-derived copper nanoparticle@carbon nanocomposites as peroxidase mimics for colorimetric sensing of asorbic aci. *Chemistry* 2014; **20**, 16377-83.

[32] NR Nirala, S Abraham, V Kumar, A Bansal, A Srivastave and PS Saxena. Colorimetric detection of cholesterol based on highly efficient peroxidase mimetic activity of graphene quantum dots. *Sensor. Actuator. B Chem.* 2015; **218**, 42-50.

[33] D Zhao, C Chen, L Lu, F Yang and X Yang. A label-free colorimetric sensor for sulfate based on the inhibition of peroxidase-like activity of systeamine-modified gold nanoparticles. *Sensor. Actuator. B Chem.* 2015; **215**, 437-44.

[34] L Xiao-Qing, D Hao-Hua, W Gang-Wei, P Hua-Ping, L Ai-Lin, L Xin-Hua, X Xing-Hua and W Chen. Platinum nanoparticles/graphene oxide hybrid with excellent peroxidase-like activity and its application for cysteine detection. *Analyst* 2015; **140**, 5251-6.

[35] F Liu, J He, M Zeng, J Hao, Q Guo, Y Song and L Wang. Cu-hemin metal-organic frameworks with peroxidase-like activity as peroxidase mimics for colorimetric sensing of glucose. *J. Nanoparticle Res.* 2016; **18**, 2-9.

[36] Q Liu, H Li, Q Zhao, R Zhu, Y Yang, Q Jia, B Bian and L Zhuo. Glucose-sensitive colorimetric sensor based on peroxidase mimics activity of porphyrin-Fe3O4 nanocomposites. *Mater. Sci. Eng. C* 2015; **41**, 142-51.

[37] P Josephy, T Eling and R Mason. The horseradish peroxidase-catalyzed oxidation of 3,5,3',5'-tetramethyl benzidine. Free radical and charge-transfer complex intermediates. *J. Biol. Chem.* 1982; **256**, 3669-75.

[38] W Lu, F Liao, Y Luo, G Chang and X sun. Hydrothermal synthesis of well stable silver nanoparticles and their application for enzymeless hydrogen peroxide detection. *Electrochim. Acta* 2011; **56**, 2295-8.

[39] M Li, Y Xiong, X Liu, X Bo, Y Zhang, C Hana and L Guo. Facile synthesis of electrospum MFe_2O_4 (M = Co, Ni, Cu, Mn) spinel nanofibers peroxide reduction. *Nanoscale* 2015; **7**, 8920-30.

[40] L Zhang, D Peng, R Liang and J Qui. Graphene quantum dots assembled with metalloporphyrins for "turn on" sensing of hydrogen peroxide and glucose. *Nanoscale* 2015; **4**, 3969-79.

[41] Y Dong, H Zhang, Z Rahman, L Su, X Chen, J Hu and X Chen. Graphene oxide-Fe_3O_4 magnetic nanocomposites with peroxidase-like activity for colorimetric detection of glucose. *Nanoscale* 2012; **4**, 3969-76.

[42] J Hao, Z Zhang, W Yang, B Lu, X Ke, B Zhang and J Tang. *In situ* controllable growth of $CoFe_2O_4$ ferrite nanocubes on graphene for colorimetric detection of hydrogen peroxide. *J. Mater. Chem. A* 2013; **1**, 4352-7.

[43] T Zhang, Y Lu and G Luo. Synthesis of hierarchical iron hydrogen phosphate crystal as a robust peroxidase mimic for stable H_2O_2 detection. *ACS Appl. Mater. Interfac.* 2014; **6**, 14433-8.

[44] J Tian, S Liu, Y Luo and X Sun. Fe(III)-based coordination polymer nanoparticles: Peroxidase-like catalytic activity and their application to hydrogen peroxide and glucose detection. *Catal. Sci. Tech.* 2012; **2**, 432-6.

[45] A Luangkhlaypho, K Pattargulwanit, N Leepipatpiboon and C Yompakdee. Development of a defined starter culture mixture of the fermentation of sato, a Thai rice-based alcoholic beverage. *Sci. Asia* 2014; **40**, 125-34.

[46] BS Chidi, FF Bauerr and D Rossouw. Organic acid metabolism and the impact of fermentation practices on wine acidity: A review. *S. Afr. J. Enology Viticulture* 2018; **39**, 1-15.

[47] H Volschenk, HJJ Vuuren and M Vjlijoen-Bloom. Malic acid in wine: Origin, function and metabolism during vinification. *S. Afr. J. Enology Viticulture* 2006; **2**, 123-36.
[48] DA Krueger. Composition of pomegranate juice. *J. AOAC Int.* 2012; **95**, 163-8.
[49] F Mizutain, T Sawaguchi and S Iijima. An interference-free, amperometric biosensor for acetic based on a tri-enzyme/polydimethysiloxane-bilayer membrane. *Chem. Lett.* 2001; **30**, 556-7.
[50] G Wen and Z Choi. Detection of ethanol in food: A new biosensor based on bacteria. *J. Food Eng.* 2013; **118**, 56-60.